UDC 616-073.756.8:616-091.8:616.1/.4:616.6/.7:616-018.002.5

Informative value of histogram analysis of digital diagnostic images

I.N. Dykan, N.N. Kolotilov

Institute of Nuclear Medicine
and Diagnostic Radiology
of the National Academy
of Medical Sciences of Ukraine, Kyiv

The well-known principle of the redundancy of any digital diagnostic image information content [1, 11] obliges to carry out these images post-processing, ensuring the extraction of patient-oriented clinically relevant information [11]. A digital image is a numerical array (voxels' matrix) of data reproducing the physicochemical and biological properties, biological objects' form and their deformation (natural for displaying all properties through 1 characteristic feature, for example, X-ray density in computed tomography), associated with methods and processes (sampling, quantization) of voxel structure CT images obtaining [9].

A lot of ways of mathematical analysis and description of image features have been developed, but the most common is the study of histogram parameters [1, 3, 5, 9]. The histogram reflects the frequency of pixels' occurrence depending on the level of their brightness [9].

The purpose of the review is to demonstrate the informative value of various options for histogram analysis of digital diagnostic images obtained with fundamentally different visualization technologies.

Sonography of hepatocellular liver cancer [7]. For post-processing on US, segmentation of areas of interest with an aperture of 64×64 pixels was performed by moving this aperture around the entire image with step in 20-pixel, and histogram was analyzed (Fig. 1, 2).

The liver echograms' texture has typically high spatial frequency, so the gradients were calculated

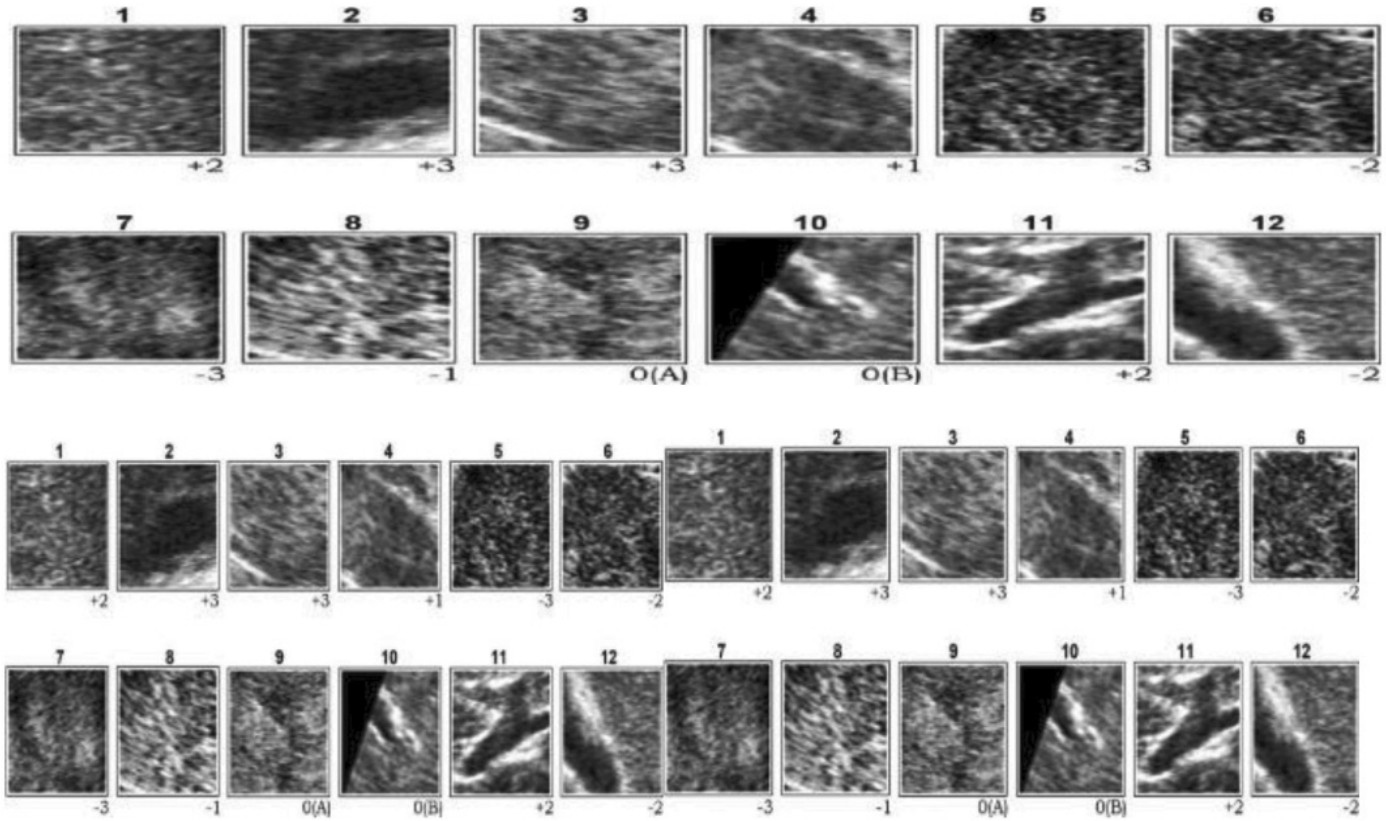

Fig. 1. *Segmentation of US liver images: 1 – border tumor-normal tissue; 2, 3, 4 – normal tissue; 5, 6 – tumor; 7 – border tumor-normal tissue; 8 – tumor [7].*

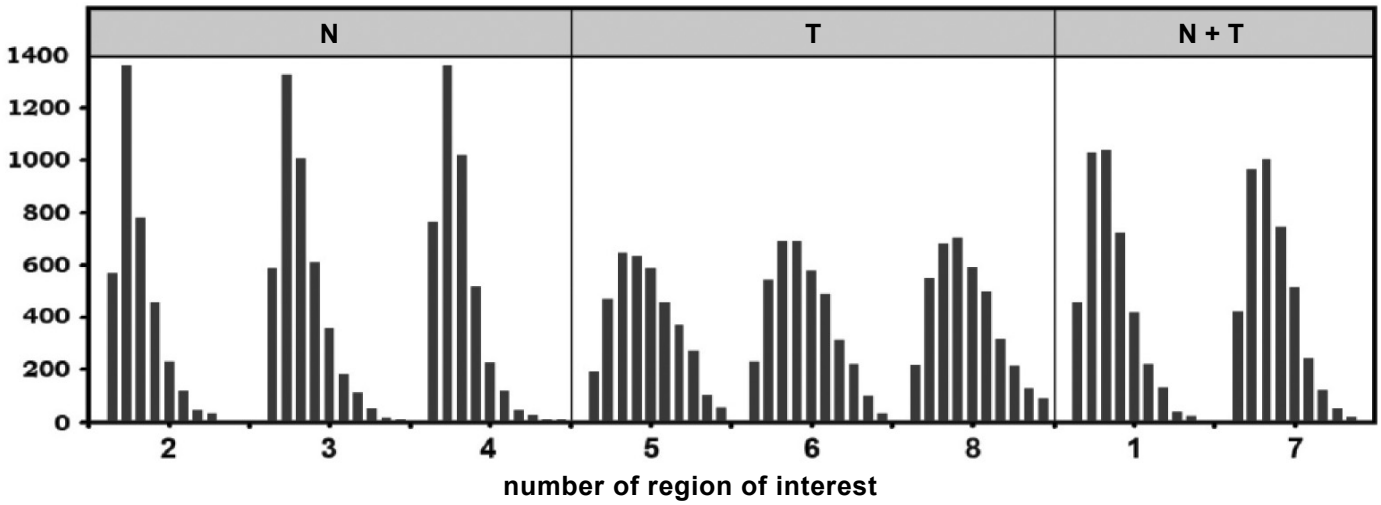

Fig. 2. *Histograms of brightness gradients (ordinate) for regions of interest 1-8 (abscissa); N – norm, T – tumor [7].*

with the classical Sobel operator (discrete differential operator calculating an approximate value of the image brightness gradient) with 3×3 window. The result of Sobel operator application at each image point is either the vector of the brightness gradient at that point, or its norm.

Local orientations were considered within the angles of 0^0-180^0, that is, the tangents' angles to the images' local structures that are perpendicular to the brightness gradients were actually considered. Accordingly, the resulting orientation histograms were symmetrical relatively the horizontal axis. Formally, orientation histograms were the vectors of the numbers W with length N:

$$W = < w_1, w_2, \ldots, w_N >,$$

where w_i – normalized to the sum the value of gradients' vectors number that fall into the azimuthal angles' sector with number i.

The number of angle intervals was taken $N = 6$, providing the necessary compromise between sensitivity (many sectors) and stability (few sectors) for an aperture of 64×64 pixels.

Typical aperture orientation histograms of the liver areas represent the "real" liver texture structure (Fig. 3).

The liver texture on the echograms has typical dominant horizontal component, which is due to the principle of a digital image based on ultrasound echo formation. As the quantitative parameter characterizing the anisotropy degree, the anisotropy coefficient was used: $k_a = \max_i (w_i)/\min (w_i)$.

The study of the orientation properties of various parts of images demonstrated that areas with tumors usually have significantly smaller values of anisotropy coefficients. Evidently, this is due to the fact that the tumor occurrence destroys the natural structure of the organ, making it less ordered and more similar to isotropic random chaos. This opinion is supported by the research results of the images' orientation properties of other organs, which demonstrate a decrease in anisotropy as the disease progresses, and during natural aging.

The results of this post-processing variant are not affected by hardly predictable pixel brightness variations (echo intensity), extremely high variability and temporal images' instability caused by the following factors as the sensor position in space, fluctuations caused by blood pulsation in blood vessels and uncontrolled changes in the degree of sensor pressure on the patient's body at manual scanning, different thickness and local features of the subcutaneous adipose tissue, all possible kinds of effects associated with ultrasonic shadows, as well as the typically high noises and the characteristic speckle images' structure.

X-ray computed tomography of pancreatic cancer [6]. Based on histogram analysis of computed tomographic images (CTI) during native, arterial, venous, delayed X-ray contrast (RC) phases of the tumor tissue, the identification method of adenocarcinoma, cystadenocarcinoma, acinarcellular cancer, undifferentiated cancer, pancreatic squamous cell carcinoma, pancreatic cancer has been developed. As a result, the application of the **clinical examination** algorithm → **(CT + RC) → post-processing CTI** provides quasi-pathological identification of 5 nosological forms of pancreatic cancer with a sensitivity of 85.2 %.

Sonoelastography (SEG) of non-epithelial tumors of the upper gastrointestinal tract [2].

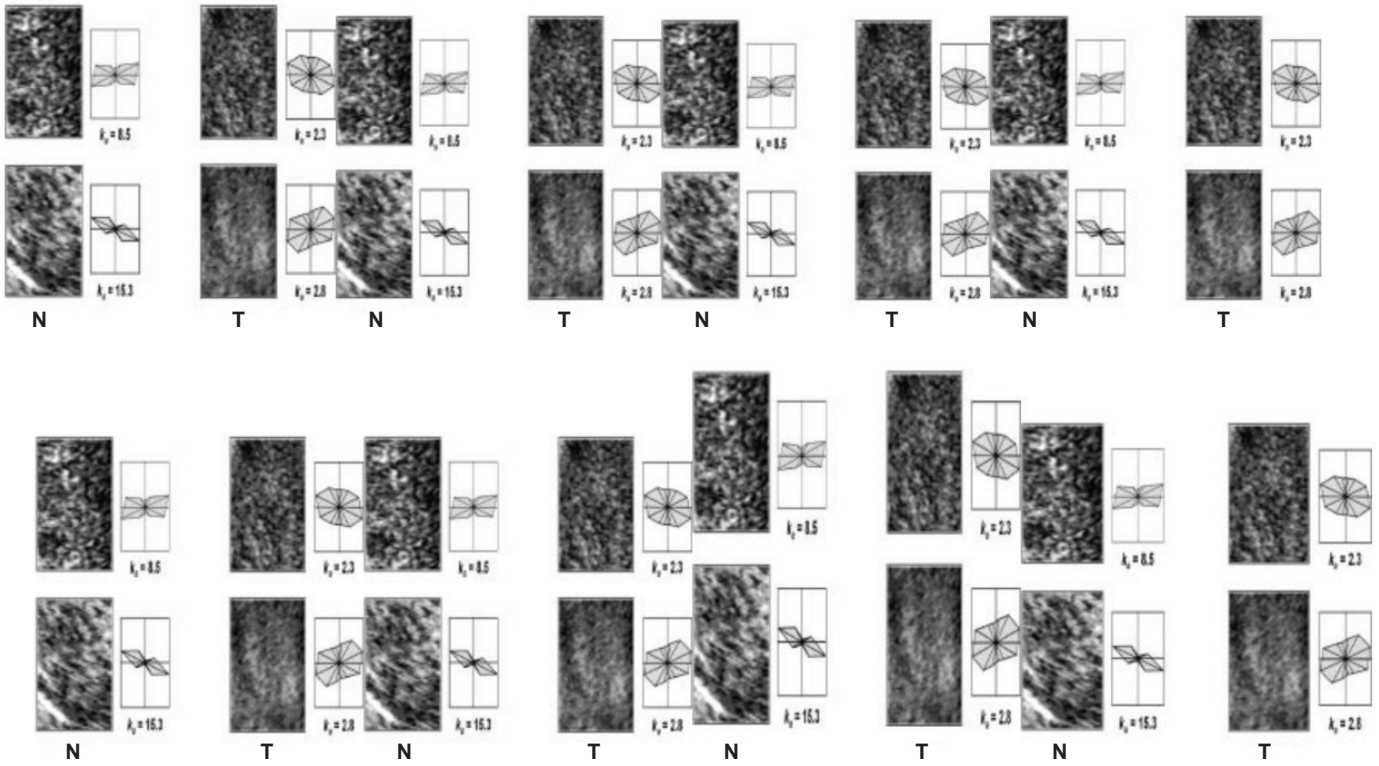

Fig. 3. *Histograms of the intact liver (1 – K^a = 7.4; 2 – K^a = 16.4) and hepatocellular carcinoma anisotropy (3 – K_a = 2.9; 4 – K^a = 3.7); N – norm, T – tumor [7].*

The histographic index I based on SEG quantitative indices was distinguished: **I = B/S+L**, where B is the histogram base width; S is the starting interval, L is the prevailing gray scale gradation (Fig. 4, 5), and the object strain factor is SR (Strain Ratio): **SR = B/A**, where A – tumor elasticity, B – adjacent intact tissues' elasticity (Table 1).

Osteoscintigraphy of breast cancer skeletal metastasis [8]. The scope of the study is 168

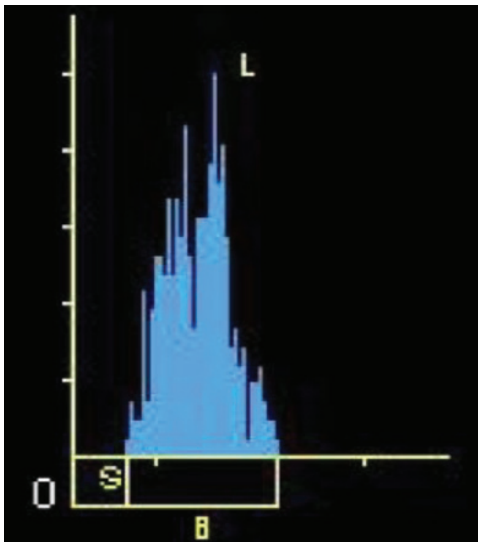

Fig. 4. *Amplitude sonohistography. B – the base of the histogram; S – the starting interval; L – the zone of the predominant grayscale [2].*

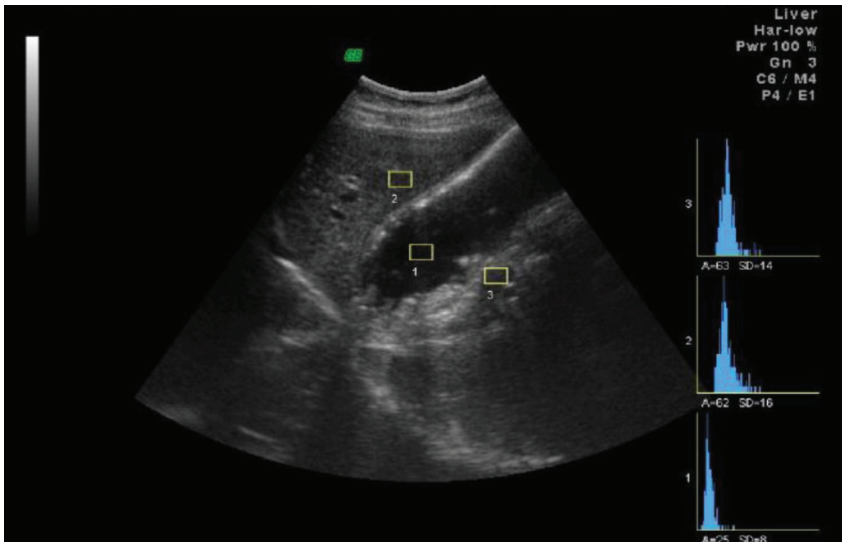

Fig. 5. *Sonohistogram variants: 1 – gastric mucosa, 2 – liver, 3 – stomach wall [2].*

Table 1.
Histographic index and tumor sonoelastography indicators.

Histological types of tumors	Index I	SR	Elasticity, кPa	Ri
Lipoma	0,34±0,03	0,48±0,11	2,6±0,54	–
Fibrolipoma	0,30±0,04	0,30±0,06	6,8±0,78	–
Leiomyoma	0,29±0,03	2,3±0,67	4,7±0,66	0,62±0,02
Lymphoma	0,23±0,04	4,7±1,24	8,2±0,83	0,48±0,06
Endophytic cancer	0,25±0,03	9,5±2,08	8,9±2,12	0,46±0,03
Gastrointestinal stromal tumors				
benign	0,35±0,04	1,2±0,88	5,9±0,76	0,54±0,05
malignant	0,22±0,03	7,8±1,91	8,5±1,93	0,48±0,01
Lymphosarcoma	0,21±0,03	11,6	9,4	0,41

breast cancer patients in the progression phase of the disease with metastases to the skeleton. The histogram parameters were calculated: average brightness, brightness smoothness, third moment of brightness, brightness homogeneity, brightness entropy.

Average brightness

$$m = \sum_{i=0}^{L-1} z_i \; p(z_i)$$

Standard deviation

$$\sigma = \sqrt{\mu_2 \; (z)} = \sqrt{\sigma^2}$$

Smoothness

$$R = 1 - 1/(1+\sigma^2)$$

Third moment

$$\mu_3 = \sum_{i=0}^{L-1} (z_i - m)^3 \; p(z_i)$$

Homogeneity

$$U = \sum_{i=0}^{L-1} p^2(z_i)$$

Entropy

$$e = -\sum_{i=0}^{L-1} p(z_i) \; log_2 \; p(z_i)$$

The differences between pathological and physiological hyperfixation foci (HFF) of the radiopharmaceutical according to histogram parameters are presented in the table below in the form of the actual values of Student's coefficient. Positive coefficients indicate the prevalence of parameter values in pathological HFF in comparison with "physiological" HFF, while negative ones – on the contrary (Table 2).

On the posterior projection of scintigrams for pathological HFF in the spine, the prevalence of the values of all indicators over similar indicators of physiological HFF is characteristic. The similar picture is observed for HFF on the anterior projection. Exception: brightness homogeneity, the differences in which between pathological and physiological HFF are unreliable. In pathological HFF in large joints on the posterior projection, there is a significant predominance of the values of the average brightness indicators, homogeneity, smoothness of the pathological foci over similar indicators of the physiological foci. In the anterior projection, the values of the average brightness and the third moment of brightness of the pathological foci significantly prevail over the similar indicators of physiological HFF.

Pathological HFF on the anterior projection in the pelvic region have significantly higher values of all histogram indices compared to physiological ones. On the posterior projection, the prevalence of mean brightness, homogeneity and entropy values in pathological HFF are significantly higher than similar values in physiological ones. On the other hand, the smoothness brightness value in physiological HFF is significantly higher than in pathological ones. Pathological HFF in the sternum region are characterized by reliable prevalence of all histogram indicators over similar indicators of physiological HFF. On

Table 2.

Indicators of histogram analysis of pathological and physiological HFF of the radiopharmaceutical on anterior planar osteosyntigrams in patients with bone metastases breast cancer [8].

Skeleton Zones	Brightness	Smoothness	3rd moment	Homogeneity	Entropy
Anterior projection					
spine	12.8	3.2	2.7	0.3	3.1
joints	24.8	6.6	2.8	–2.1	0.8
pelvis	24.9	10.0	6.5	6.5	11.9
sternum	20.4	8.1	6.5	15.2	15.8
long tubular bones	3.6	4.2	4.4	12.9	12.4
subordinate sinuses	6.5	0.8	0.6	11.1	–10.2
skull	13.3	5.8	1.9	2.8	3.7
chest	15.4	7.7	3.8	–3.6	–4.8
Posterior projection					
spine	26.9	7.3	4.8	3.2	4.3
joints	10.6	3.8	1.1	–4.3	–1.8
pelvis	24.6	–4.7	–2.3	11.4	9.6
long tubular bones	2.1	–3.2	0.3	–1.8	–2.2
scull	13.2	3.7	–0.01	1.3	2.6
chest	11.3	–1.9	–1.2	0.01	–4.1

the anterior projection of scintigrams, pathological HFF in long tubular bones are distinguished by reliably high values of all histogram values compared with physiological HFF. In the posterior projection, the differences between the parameters of both groups of HFF are not significant. The exception is only the indicator of brightness smoothness. Its values for physiological HFF were reliably higher than those in pathological foci. Pathological foci in the paranasal sinuses were characterized by significantly high average brightness and homogeneity, and physiological – by high entropy value.

Magnetic resonance imaging of meninges tumors [10]. Preoperative verification of the histological subtype and density of the meninges tumors affect the approaches and predictions of surgical intervention. In this work, an integral histogram (summarized from all T_1WI with contrast enhancement) in the tumor volume with subsequent comparison with histological diagnosis was calculated. Before graphic construction of the histogram, the relative intensity of the MR signal of each voxel in the tumor was calculated. The signal intensity in the tumor was normalized by the brain white matter, taking into account the histogram shift coefficient relative to the intact white matter (Fig. 6, 7).

Sonography at chronic pancreatitis [4]. The pancreas and its parts' sizes (head, body, tail), the contours clarity, the structure homogeneity, echogenicity, the pancreatic duct diameter, the presence of pseudocyst, calcifications were investigated in patients with chronic pancreatitis.

Additionally, ultrasound histography was performed in the area of the pancreas head with the evaluation of *L, N, Kgst* indicators for the results' objectification: its *L, M, T* indicators are automatically displayed on the screen next to the histogram (Fig. 8).

With increasing echogenicity, *L* indicator increases, and it decreases with decreasing. For example, with respect to the pancreas, the *L* indicator increases at fibrosis, fatty degeneration, etc. The decrease of *L* can be expected in cases of pancreatic edema (for example, at acute pancreatitis).

For the analysis of histograms additionally two indicators were developed. The Homogeneity index is calculated with the following formula:

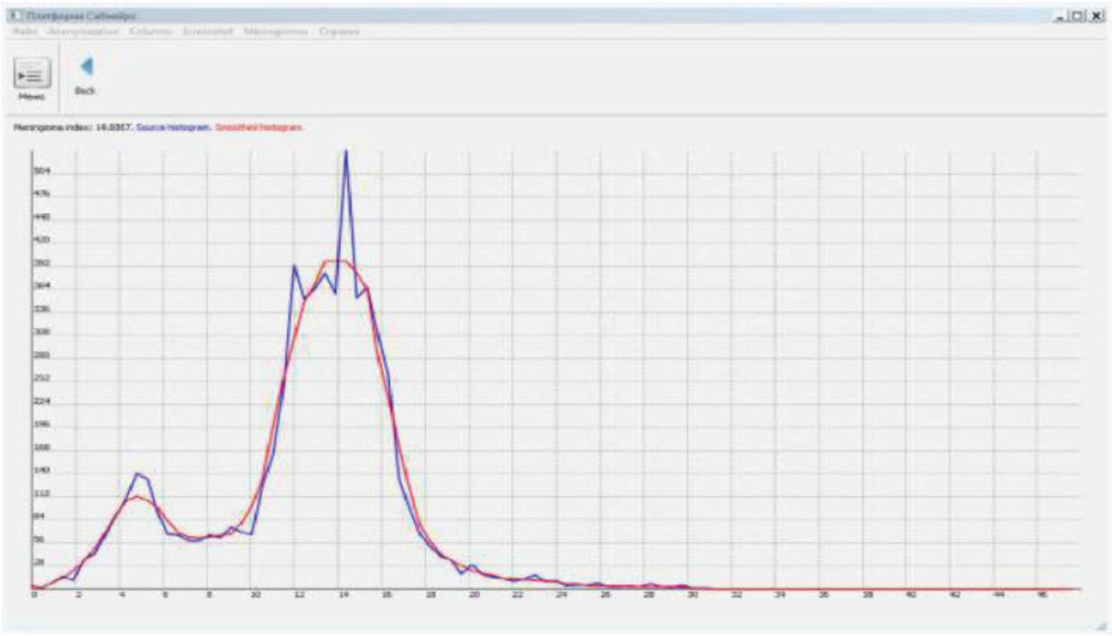

Fig. 6. *Histogram for meningothelial type of tumor [10].*

N=(M/T)- 100%, where *N* is the indicator of pancreas tissue homogeneity, *M* is the number of the shadow component elements, which occurs more often than others in the given area, *T* is the total number of elements in the given area.

The histographic coefficient *Kgst* is calculated using the following formula: **Kgst = (N/P•L)• 10 000**, where *N* is the homogeneity indicator of the pancreas tissue, *P* is the maximum grayness level in this histogram (see Fig. 8), *L* is the grayness level, which is the most common in this area.

The proposed indicators (*N, Kgst*) allowed to increase the informative value of pancreas US in patients with chronic pancreatitis (sensitivity up to 85 % and specificity up to 81 %), whereas the sensitivity of traditional pancreas US, according to our data, was 72 % and specificity – 68 %.

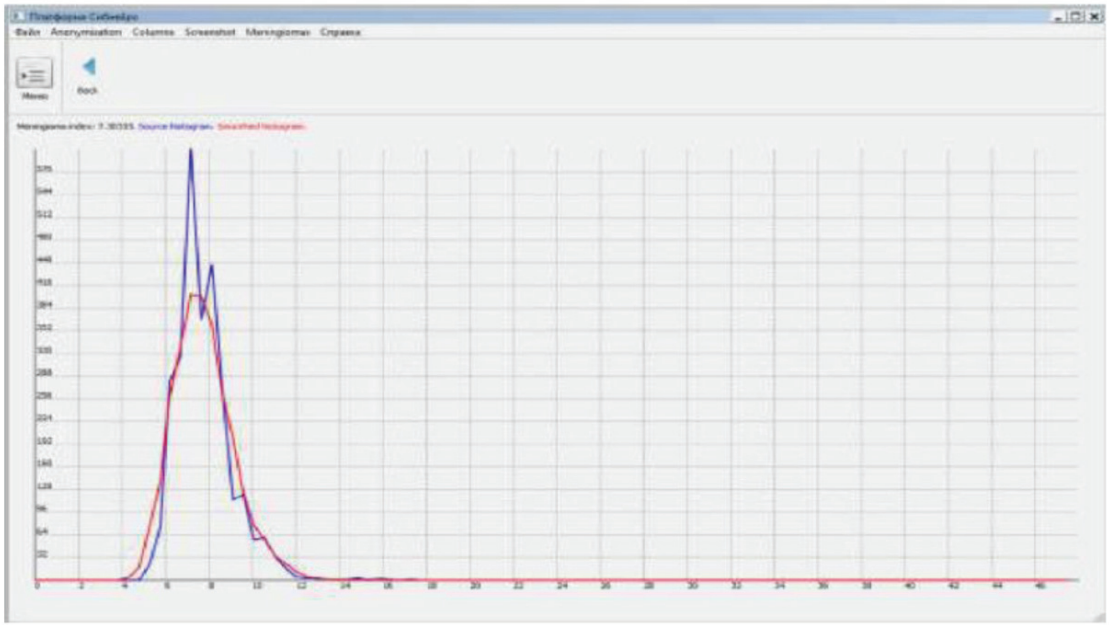

Fig. 7. *Histogram for anaplastic/atypical type of meningioma [10].*

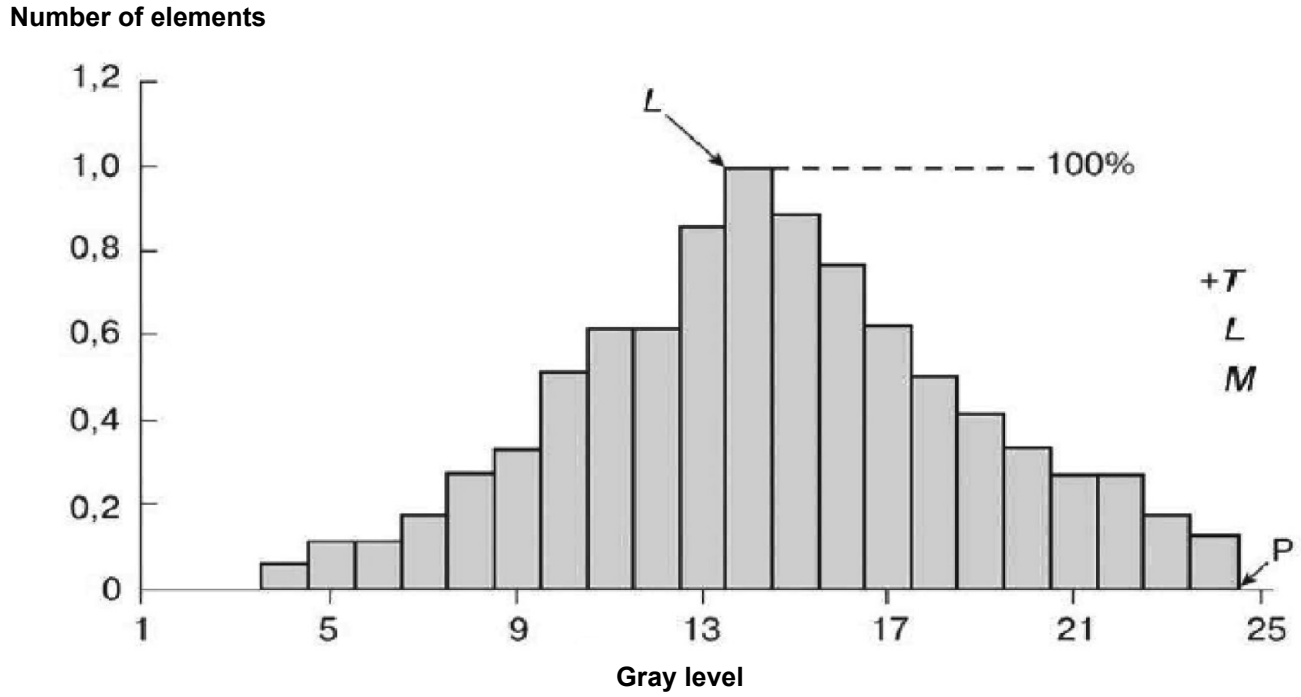

Fig. 8. *Histogram of echogram: by ordinate – number of pixels; by abscissa – gray level; T – the total number of elements in the additional or fixed area; L – the scale level of the gray shadow component, which is the most common in a particular area; M – the number of elements of the shadow component, which is the most common in a particular area; P – maximum grayness level in the histogram [4].*

Conclusion

The values of the histogram parameters, along with the brightness, contrast, shape and homogeneity of the foci structure, are the informative diagnostic signs of the particular pathology on the diagnostic images and can contribute to the correct pre-operative express diagnostics.

Literature

1. Автандилов Г. Г. Медицинская морфометрия: руководство / Г. Г. Автандилов. − М.: Медицина,1990. – 384 с.

2. Алиева И. М. Возможности лучевых методов исследования и эндоскопии в диагностике неэпителиальных новообразований верхних отделов желудочно-кишечного тракта: диссертация ... кандидата медицинских наук: 14.01.13 / Алиева Ильмира Марсовна; [Казанская государственная медицинская академия]. – Казань, 2015. – 111 с.

3. Бабкіна Т. М. Впровадження в комп'ютерну томографію гістографічного аналізу пухлин головного мозку / Т. М. Бабкіна, М. М. Колотілов, В. О. Рогожин // Одеський мед. журнал. − 2002. − № 5. − С. 26-28.

4. Губергриц Н. Б. Возможности ультразвуковой гистографии в оценке выраженности фиброза поджелудочной железы при хроническом панкреатите / Н. Б. Губергриц, В. Я. Колкина // Терапевтический архив. – 2015. – № 2. – С. 59-63.

5. Дикан І. М. Диференціальна діагностика синоназальних захворювань із застосуванням мультидетекторної комп`ютерної томографії за кількісними ознаками / І. М. Дикан, Ю. П. Терницька // Лучевая диагностика, лучевая терапия. – 2013. – № 2-3. – С. 46-56.

6. Забудская Л. Р. Злокачественные опухоли поджелудочной железы: постпроцессинг компьютерно-томографических нативных и рентгеноконтрастированных изображений / Л. Р. Забудская //Лучевая диагностика. Лучевая терапия. – 2016. – № 3. – С. 82-86.

7. Ковалев В. А. Распознавание опухолей на ультразвуковых изображениях печени с использованием решающих правил / В. А. Ковалев // Информатика. – 2016. − № 2. – С. 59-70.

8. Косых Н. Э. Компьютерный автоматизированный анализ в задачах распознавания медицинских изображений на примере сцинтиграфии / Н. Э. Косых, Н. М. Свиридов, С. З. Савин, Т. П. Потапова // Компьютерные ис-

следования и моделирование. – 2016. – Т. 8, № 3. – С. 541-548.

9. Розенфельд Л. Г. Возможности постобработки диагностических КТ - и МРТ-изображений на персональном компьютере / Л. Г. Розенфельд, Н. М. Макомела, Н. Н. Колотилов // Український медичний часопис. − 2006. − № 6 (56). − С. 69-73.

10. Сергеев Г. С. Программное планирование и прогнозирование эффективности хирургического лечения опухолей головного мозга: диссертация ... кандидата мед. наук: 14.01.18 / Глеб Сергеевич Сергеев; [Военно-медицинская академия]. – 2018. – 109 с.

11. Терновой К. С. Принципы решения медицинских проблем / К. С. Терновой, Л. Г. Розенфельд, Н. К. Терновой, Н. Н. Колотилов // – К.: Наук. думка, 1990. – 220 с.

INFORMATIVE VALUE OF HISTOGRAM ANALYSIS OF DIGITAL DIAGNOSTIC IMAGES

I.N. Dykan, N.N. Kolotilov

The purpose of the review is to demonstrate the informative value of various options of histogram analysis of digital diagnostic images obtained with fundamentally different visualization technologies.

The informativeness of diagnostic imaging histogram analysis at hepatocellular liver cancer US investigation, pancreas cancer X-ray Computed Tomography, non-epithelial tumors of the upper gastrointestinal tract sonoelastography, osteoscintigraphy of breast cancer bone skeletal metastases, brain membranes tumors MRI, echography at chronic pancreatitis was described.

The values of the histogram parameters, along with the brightness, contrast, shape and homogeneity of the foci,structure are the significant diagnostic signs of the particular pathology on the diagnostic images and can contribute to the correct pre-operative express diagnostics.

ІНФОРМАТИВНІСТЬ ГІСТОГРАМНОГО АНАЛІЗУ ЦИФРОВИХ ДІАГНОСТИЧНИХ ЗОБРАЖЕНЬ

І.М. Дикан, М.М. Колотілов

Мета огляду – показати інформативність різних варіантів гістограмного аналізу отриманих за принципово різними технологіями візуалізації цифрових діагностичних зображень.

Описана інформативність гістограмного аналізу діагностичних зображень при ехографії гепатоцелюллярного раку печінки, рентгенівської комп'ютерної томографії ракових пухлин підшлункової залози, соноеластографії неепітеліальних пухлин верхніх відділів шлунково-кишкового тракту, остеосцинтиграфії скелетних метастазів раку молочної залози, магнітно-резонансної томографії пухлин оболонок головного мозку, ехографії при хронічному панкреатиті.

Значення гістограмного параметрів, поряд з яскравістю, контрастністю, формою і гомогенністю структури осередків, є значущими діагностичними ознаками тієї чи іншої патології на діагностичних зображеннях і можуть сприяти коректної доопераційної експрес - діагностики.

ИНФОРМАТИВНОСТЬ ГИСТОГРАММНОГО АНАЛИЗА ЦИФРОВЫХ ДИАГНОСТИЧЕСКИХ ИЗОБРАЖЕНИЙ

И.Н. Дыкан, Н.Н. Колотилов

Цель обзора – показать информативность различных вариантов гистограммного анализа полученных по принципиально разным технологиям визуализации цифровых диагностических изображений.

Описана информативность гистограммного анализа диагностических изображений при эхографии гепатоцелюллярного рака печени, рентгеновской компьютерной томографии раковых опухолей поджелудочной железы, соноэластографии неэпителиальных опухолей верхних отделов желудочно-кишечного тракта, остеосцинтиграфии скелетных метастазов рака молочной железы, магнитно – резонансной томографии опухолей оболочек головного мозга, эхографии при хроническом панкреатите.

Значения гистограммных параметров, наряду с яркостью, контрастностью, формой и гомогенностью структуры очагов, являются значимыми диагностическими признаками той или иной патологии на диагностических изображениях и могут способствовать корректной дооперационной экспресс − диагностике.